



Experimental Analysis of Bending Resistance of Bamboo Composite I-Shaped Beam

Wenqing Wu, M.ASCE¹

Abstract: A new type of bamboo composite I-shaped beam, which consists of bamboo laminate as its upper and down flange plates and bamboo curtain plywood as its web, was introduced in the paper. In this new type of beam, a connection between the flange plates and the web was enabled with a combined action of epoxy resin adhesive and a bolting joint. A model test on the bending mechanical properties (e.g., bending failure mode and bending capacity) and the factors influencing the flexural rigidity of the bamboo composite I-shaped beam was conducted. The preliminary results showed that the bamboo composite I-shaped beam has excellent mechanical properties that could offer high bending capacity and bending rigidity, as well as excellent ductility of the structure. Therefore, the bamboo composite I-shaped beam is potentially interesting for application in small- to medium-span bridges as a new type of structure. Moreover, this experimental research could help with a design method for bamboo composite I-shaped beams in the future. DOI: [10.1061/\(ASCE\)BE.1943-5592.0000557](https://doi.org/10.1061/(ASCE)BE.1943-5592.0000557). © 2013 American Society of Civil Engineers.

Author keywords: Bamboo composite material; Bamboo strip-laminated board; Bamboo curtain plywood; I-shaped beam; Bending resistance.

Introduction

Building materials are commonly selected through functional, technical, and financial requirements. However, with sustainability as a key issue in the last decades, especially in western countries, the environmental load of building materials has now also become an important criterion (Van der Lugt et al. 2006). The building industry, directly or indirectly causing a considerable part of annual environmental damage, has to take more responsibility to contribute to sustainable development by finding more environmentally benign ways of construction and building. One of the directions for solutions is to be found in new material applications: recycling and reuse, sustainable production of products, or use of renewable resources. Bamboo, as a fast growing renewable material with a simple production process, is expected to be a sustainable alternative for more traditional structural materials, such as concrete, steel, and timber (Van der Lugt et al. 2006; Janssen 1981).

The bamboo species and bamboo planting areas in China account for approximately 1/4 of those in the world. In addition, bamboo production in China accounts for approximately one-third that of the world and ranks first worldwide. Bamboo has an excellent physical performance and better mechanical properties compared with current traditional construction materials (Ahmad and Kamke 2005; Bahari et al. 2010). Test results provided by Yu et al. (2008) indicated that the longitudinal elastic modulus and the tensile strength of Moso bamboo depends on the radial position, the elastic modulus, and the tensile strength at the outer layer (with an average of 26.9 GPa and 295.6 MPa, respectively) were almost triple those of the inner layer (with an average of 9.7 GPa and 113.4 MPa, respectively), and the strength-to-weight ratio of bamboo is three to

four times that of steel. Most notably, it is highly renewable, because bamboo stalks reach maturity in just 8 years. As such, it makes an appealing candidate as a structural material. With adequate research, it is conceivable that bamboo could become a sustainable alternative to current building materials in China, North America, and other western countries (Van der Lugt et al. 2006; Lee et al. 1994; Rittironk and Elnieiri 2008; Nath et al. 2009).

Bamboo, being a hollow tube, is efficient in resisting bending forces, with a large ratio of moment of inertia to cross-sectional area. It is difficult, however, to create connections for this shape, and tubes cannot be used in applications where flat surfaces are required.

Bamboo-based boards such as bamboo strip laminated plywood have been produced in China and in other countries by using adhesive to join bamboo strips taken from the culm (i.e., bamboo stem) (Gao et al. 2008; Jorissen et al. 2007). The bamboo production of composite bamboo-based boards, having highly renewable characteristics and better physical and mechanical properties than that of crude bamboo, is more competitive compared with traditional building materials commonly used, such as steel and concrete (Zhang and Yue 2004; Sun et al. 2008; Sulastiningsih and Nurwati 2009).

The mechanical properties of bamboo-based boards are mainly divided into tensile strength parallel to the grain, compressive strength parallel to the grain, static bending strength parallel to the grain, shear strength parallel to the grain, and modulus of elasticity. Table 1 shows a performance comparison between bamboo plywood and several types of wood (Gao et al. 2008; Zhang and He 2007; Yu et al. 2006). As shown in Table 1, the bending strength parallel to the grain of *Dendrocalamus giganteus* bamboo can achieve more than 200 MPa, and the modulus of elasticity is more than 20 GPa, which is higher than that of ordinary wood materials such as Korean pine. The compressive strength and tensile strength of Moso bamboo-based boards are close to that of wood.

In the United States and other countries, however, bamboo production is not officially recognized as a structural building material because of the absence of any standard building codes, which prevents it from being freely accepted by the construction industry. It is mainly used for nonstructural applications such as flooring, fencing, furniture and crafts, and ornamental purposes. To have

¹Professor and Head, Dept. of Bridge Engineering, Southeast Univ., Nanjing 210096, China. E-mail: wqwuxu@hotmail.com

Note. This manuscript was submitted on January 10, 2013; approved on September 16, 2013; published online on September 19, 2013. Discussion period open until May 11, 2014; separate discussions must be submitted for individual papers. This paper is part of the *Journal of Bridge Engineering*, © ASCE, ISSN 1084-0702/04013014(13)/\$25.00.

Table 1. Performance Comparison between Bamboo Plywood and Other Types of Wood Material

Material	Bending strength (MPa)	Bending elastic modulus (GPa)	Compressive strength parallel to grain (MPa)	Compressive strength perpendicular to grain (MPa)	Tensile strength parallel to grain (MPa)
Moso bamboo-laminated plywood ^a	136.8	10.62	85.47	36.5	137
Moso bamboo-curtain plywood ^a	121.3	11.95	71.99	65.62	91.7
<i>Dendrocalamus giganteus</i> -laminated plywood ^b	210.2	23.48	89.05	—	—
Dahurian larch ^c	113.3	14.5	—	46	129.9
Korean pine ^c	65.3	10	—	37	98.1

^aGao et al. (2008).^bYu et al. (2006).^cZhang and He (2007).

bamboo production be selected more commonly as a structural material, much research is still needed. This change will constitute the major goal and the challenge in the innovation and reform of civil engineering in the 21st century (Shan et al. 2009; Shen et al. 2009; Wei et al. 2011). Thus far, the application-oriented study of bamboo as a structural material has been carried out for a long time in China and other countries (Xiao et al. 2010, 2012; Van der Lugt et al. 2006; Lee et al. 1994; Rittironk and Elnieiri 2008; Nath et al. 2009; Amino 2004, 2005).

Based on the excellent physical and mechanical properties of bamboo-based boards, a new type of bamboo composite I-shaped beam structure is presented in this paper. This new structure can be used as an alternative load-bearing structure for medium-span and small-span bridges. In this paper, the bamboo composite materials used are bamboo strip-laminated board and bamboo curtain plywood. The former is made of glued and compressed unidirectional bamboo strips, with high compressive strength parallel to the grain. The latter is made of glued and compressed orthogonal bamboo strips, with relatively high compressive strengths parallel to the grain and perpendicular to the grain (Gao et al. 2008). The bamboo strip-laminated board is termed as a grade I board (M_1), and the bamboo curtain plywood is termed as a grade II board (M_2). To make full use of the respective strength characteristics of the two types of bamboo-based boards, grade I boards are used for top and bottom flange plates of the I-shaped beam, and grade II boards are used for the web. The cross section of the bamboo composite I-shaped beam was composed of three pieces of bamboo plywood fabricated by a certain connection technology. The connection between the top/bottom flanges and the web relies on the combined use of epoxy resin structural adhesive and mechanical bolts. In this research, a series of experiments with four test beams was carried out on the bending resistance of the bamboo composite I-shaped beam to study the bending failure mode, bending capacity, and influential factors of the bending rigidity. The results of the current study may serve as a theoretical basis for a structural design method of bamboo composite beams.

Test Overview

Of four test beams in total, external longitudinal steel reinforcement was applied on two of them, wherein one was subjected to external prestress to study the influence of prestressing on the mechanical property of bamboo I-shaped beam.

The purpose of adding the external prestressing reinforcement in the bamboo composite structure is to investigate the effect of external reinforced bars and external prestressing on the stiffness and the load-bearing capacity of the bamboo composite structure. There

is also research related to the practice of similar studies on timber structures, which was introduced first in Netherlands in 1970s and, most recently, in New Zealand (Buchanan et al. 2008; Smith et al. 2008). Structural members made of laminated veneer lumber (LVL) in combination with unbonded posttensioning have recently been proposed in New Zealand, which makes it possible to design moment-resisting frames with longer spans for multistory timber buildings. Moreover, prefabricated and prestressed timber buildings can be designed to have enhanced recentering and energy dissipation characteristics for seismic resistance (Iqbal et al. 2008).

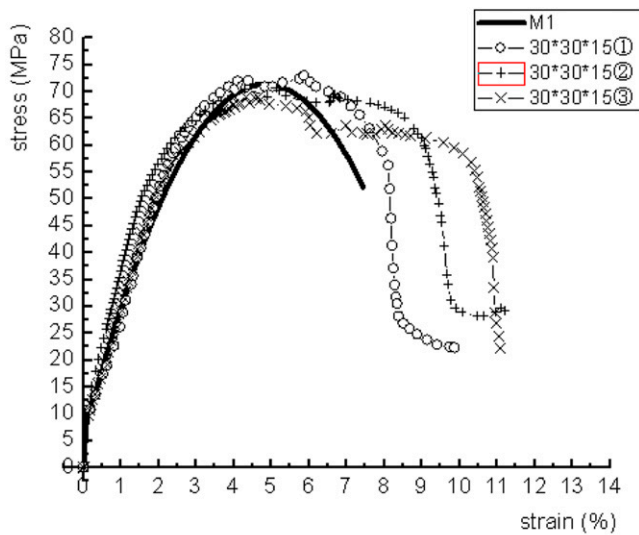
Test Materials

The bamboo-based boards were produced by Zhong'ao Bamboo Plywood Factory (Anji County, Zhejiang Province, China). The grade I bamboo-based board (M_1) used for top and bottom flange plates was 2,440 mm in length, 200 mm in width, and 15 mm in thickness, with a tensile strength parallel to the grain of 127 MPa and a compressive strength parallel to the grain of 53.5 MPa. The grade II bamboo-based board (M_2) used for the web was 2,440 mm in length, 270 mm in width, and 15 mm in thickness, with a tensile strength parallel to the grain of 79 MPa and a compressive strength parallel to the grain of 35.8 MPa (Wu et al. 2012a, b, c). The complete stress-strain diagram of the two composite materials in compression is shown in Fig. 1. All data mentioned previously are the pure material properties obtained by testing small specimens. The external tendon was a prestressing steel wire with a diameter of 5 mm and a design tensile strength of 1,570 MPa; the grade of the connecting angle steel plate was Q235 in China standard (National Standard of Peoples Republic of China 2001), and the design tensile strength was 235 MPa. The diameter of the connecting bolt was 8 mm, the level of material performance was Grade 5.6, the nominal tensile strength was 500 MPa, the nominal yield strength was 300 MPa, and the length of the bolts were 45, 50, and 55 mm, respectively. The adhesive glue was a polyacrylate rubber modified epoxy resin structural adhesive with a standard shear strength of 4 MPa.

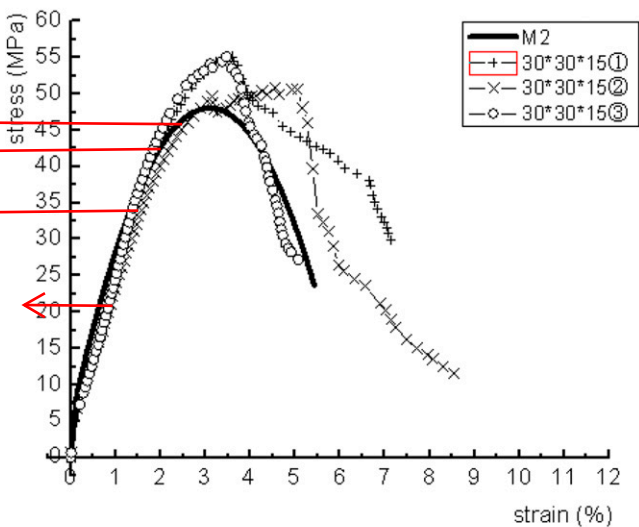
Because material properties and fabrication practices may differ, values reported herein may or may not be representative of those that would be obtained for larger samples made by others.

Design of the Test Beam

As shown in Fig. 2, the test specimens were a simply supported beam. The specimens were 2.44 m in total length, 0.3 m in depth, and 0.2 m in width. The calculated span of the beam was 2.14 m. The web and flange plates of the I-shaped beam were all 15 mm in thickness.



(a) curves for bamboo strip-laminated board



(b) curves for bamboo curtain plywood

Fig. 1. Complete stress-strain curves of two composite materials in compression: (a) curves for bamboo strip-laminated board; (b) curves for bamboo curtain plywood

Four diaphragm plates with a thickness of 30 mm were installed along the longitudinal direction of the beam.

With respect to the fastening method, three components including one piece of web and two piece of flanges for each I-shaped beam were mechanically joined by bolts first and then supplemented with bonding (Fig. 3). The kind of composite joint mode was deemed as reliable; the related research results showed that the high stiffness and bending strength of composite I-shaped beam could be gained by a combination joints of mechanical nails and structural adhesive (Kumar et al. 1972; Leichti et al. 1990; Bohnhoff and Siegel 1991).

The flange-web joint was provided by mechanical bolts at 13 cross sections along the longitudinal direction of the test beam (Fig. 2), and the same connecting way was also used in the flange-diaphragm joint. Prior to when the previous operating steps were finished, the contact areas of the flange-web joint and the flange-diaphragm joint should be cleaned first and then applied along the contract area by epoxy structural adhesive; hereafter, all components of the I-shaped beam could be joined by mechanical bolts to generate

a pressure between the joint areas, which could be helpful for increasing the bonding action of the structural adhesive. After all operating steps were finished, all components of the composite beam were well connected by mechanical bolts and structural adhesive.

Four test beams were used and named as Beams 1–4, respectively, of which Beams 1 and 2 were the beams without reinforcement [Fig. 2(a)], whereas Beams 3 and 4 were equipped with two external steel rebars ($2@ \phi^W 5$) of high-strength steel wire [Fig. 2(b)]. Beam 3 was subjected to external prestressing, with a tensile force of 22 kN for each external rebar, whereas Beam 4 was only equipped with two external rebars but without external prestressing. The details of the steel tube as a deviating device for external tendons are shown in Fig. 2(c).

Test Condition

The four-point concentrated loading method was adopted for each test beam, as shown in Fig. 4. In the test, Beam 1 was loaded under a loading increment of 4 kN, whereas Beams 2–4 were loaded under a loading increment of 2 kN in each loading step until the beam structure was damaged. The loading-time curves for four tested beams are shown in Fig. 5. A strain gauge and dial indicator were installed at the key cross sections to measure the strain and deformation of the beam (Fig. 4).

The criteria for judging the beam failure in the test were as follows: the flange plates or the web of the I-shaped beam are fractured or torn apart, the beam is deformed seriously, or the principal connection between the flange and web fails.

Analysis on Test Results of Failure Mode and Failure Load

The failure mode of the four test beams are shown in Fig. 6. Details of the failure mode, failure types, and failure loads are shown in Table 2.

Table 2 shows that Beam 3 with prestressed rebars is destroyed by loss of stability at the upper half of the web and that all other beams are damaged by material tearing. The cracking direction is perpendicular to the glue line on the lower flange-web joint.

The test results also show that the bolted connection easily causes local stress concentration and leads to material tearing failure. In this study, material tearing failure can be attributed to the fact that the number of bolted connections is limited, and the stress concentration on the connections is obvious. Increasing the number of connecting bolts and optimizing the distribution of mechanical bolts along the flange-web joints would be considered as an effective way to improve the local stress state mentioned previously.

Both Beams 1 and 2 without reinforcement have the same configuration, but the bending capacity of Beam 1 is slightly lower than that of Beam 2. The possible reason of causing the difference in bending capacity is that the loading increment on Beam 1 was twice as great as that on Beam 2, leading to some adverse effects on the bearing capacity of Beam 1.

No significant difference can be observed in bending capacity between Beams 3 and 4 with reinforcement and Beams 1 and 2 without reinforcement, which indicates that external reinforcement or even external prestressing cannot effectively improve the bending capacity of the beam. However, the failure mode of Beam 3 was changed to web buckling failure instead of material tearing failure because of the action of the external prestressing. Thus, the external prestressing is considered to be beneficial for optimizing the local stress state of the structure.

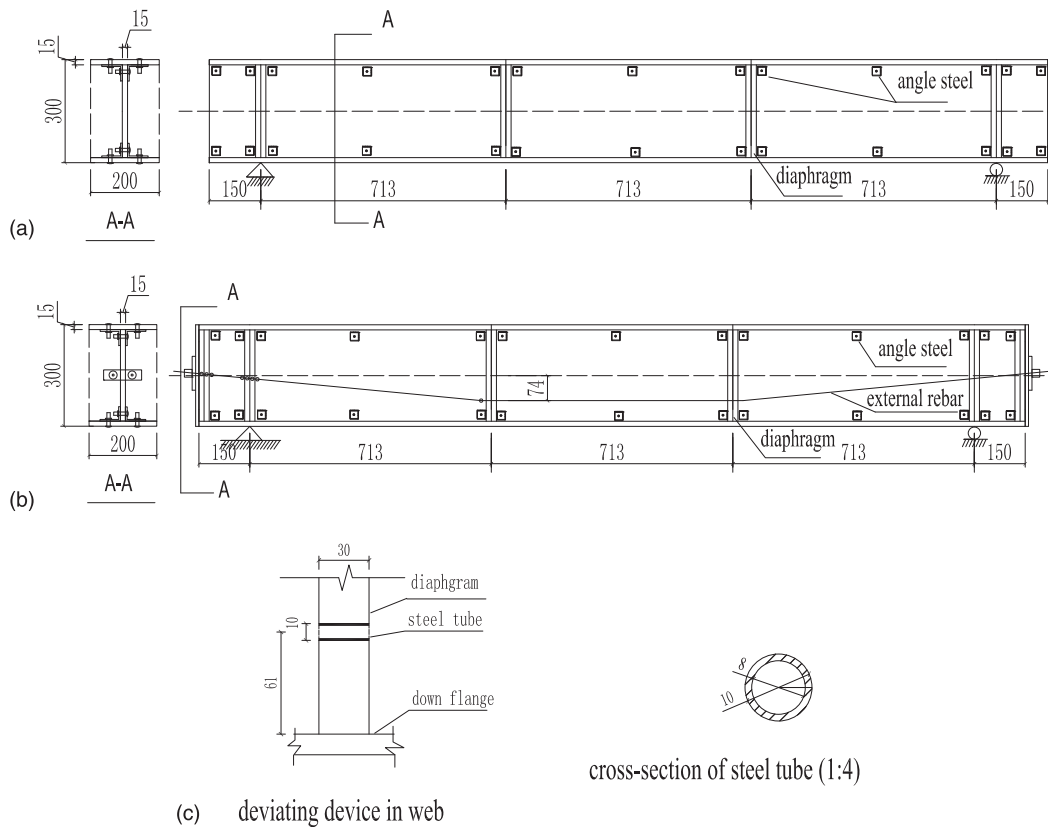


Fig. 2. Specimen configuration of bamboo composite I-shaped beam (mm): (a) configuration of I-shaped bamboo beam without reinforcement (mm); (b) configuration of I-shaped bamboo beam with reinforcement (mm); (c) detail of steel tube as deviating device for external tendon (cm)

Effect of Connecting Way on the Structural Deflection

The typical deformation state of test beam failure is shown in Fig. 7. As shown in Fig. 7, the test beam seems to be of high ductility because of its larger deformation on beam failure.

The loading-deformation experimental curves of the test beams are shown in Fig. 8. Fig. 8 shows that the midspan deflection curves of the four beams undergoes a linear phase and a subsequent nonlinear phase as the applied load increases. The phase classification of the loading-deflection experimental curves of the four beams is shown in Table 3. The loading-deflection curve shows that the variation range of deformation is small in the linear phase, but the structural deformation mostly occurred in the subsequent nonlinear phase.

For the analysis on the relation between the structural deformation and the flange-web connecting way, the structural deformation of the test beam was analyzed with two working conditions by finite-element models (FEMs) before the test started (Ma 2013). The FEM of Beams 1 and 2 is shown in Fig. 9.

The FEM software used was *ANSYS*, version 10.0. The major parameters related with FEM are illustrated in the test materials mentioned previously. The major details of FEM are described simply as follows: all data were cited from a related master's thesis under the supervision by the author (Ma 2013). Each FEM of the flanges and the web was meshed using 10-node tetrahedral structural solid elements, which are well suited for meshing irregular geometries. Elements were typically sized to a maximum edge length of 25 mm. The flange-web connection is modeled by spring type elements to stimulate the shear flexibility of each bolted joint, and the shear flexibility results from the embedding stress behavior of bamboo material under a bolt shank, which is one of the sources of nonlinearity in the loading-deflection curves (Fig. 10). The embedding behavior

parallel to the grain was assumed to be perfectly elastic-plastic; that is, it behaves linearly up to an embedding yield strength and then is constant after the yielding. The connection spring stiffness k_s , equal to 26.5 GPa/m, was obtained from the literature (Sawata and Yasumura 2003), because there is no related data for the bamboo bolted-connection stiffness until now. The structural bonding along the flange-web glue line was simulated by the contact element.

There are two connection modes of the flange-web joint to be simulated in this work, including one deformable connection and another assumed rigid connection; the former connection is mentioned previously, and the latter one is considered with the full composite action of the flange-web joint. The rigid connection of the flange-web joint is simulated by coupling all the nodes located along the contact area between the flange and web. All the material parameters used in the FEM are the same as those for the test beams. There are 8,856 elements and a total of 18,058 nodes in the FEM.

The failure criteria assumed for bamboo components are the Tsai-Wu failure criterion, which is widely used for anisotropic composite materials and presented as the following (Tsai and Wu 1971):

$$F_i \sigma_i + F_{ij} \sigma_i \sigma_j = 1 \quad i, j = 1, \dots, 6 \quad (1)$$

where F_i and F_{ij} = strength tensors; σ_i and σ_j = normal stresses when i and j equal 1, 2, or 3; and σ_i and σ_j = shear stresses when i and j equal 4, 5, or 6.

The failure criteria assumed for the glued connection are that the shear stress at a certain position along the glue line of the flange-web joint exceeds the critical value of 4 MPa, and then local crack failure would occur, and its failure load based on the FE analyses (FEAs) could be approximately predicted.

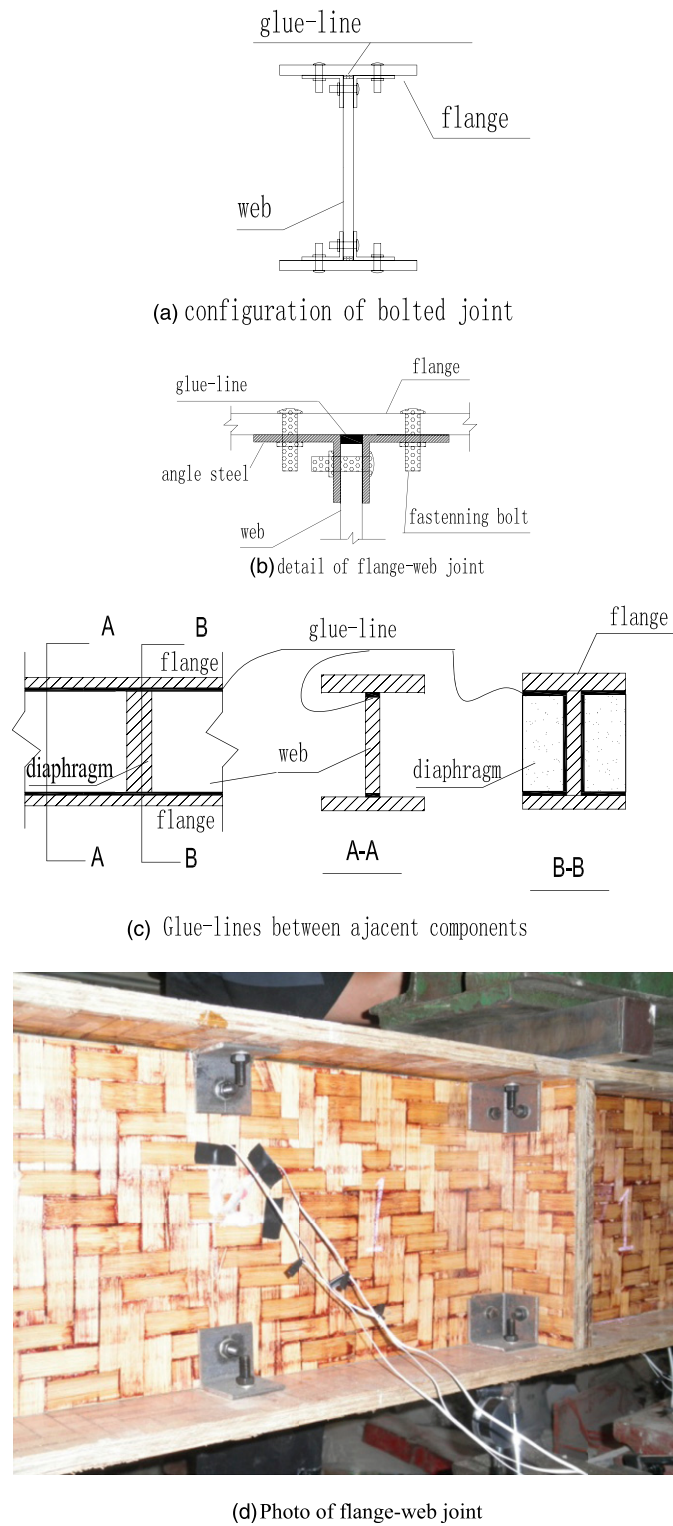
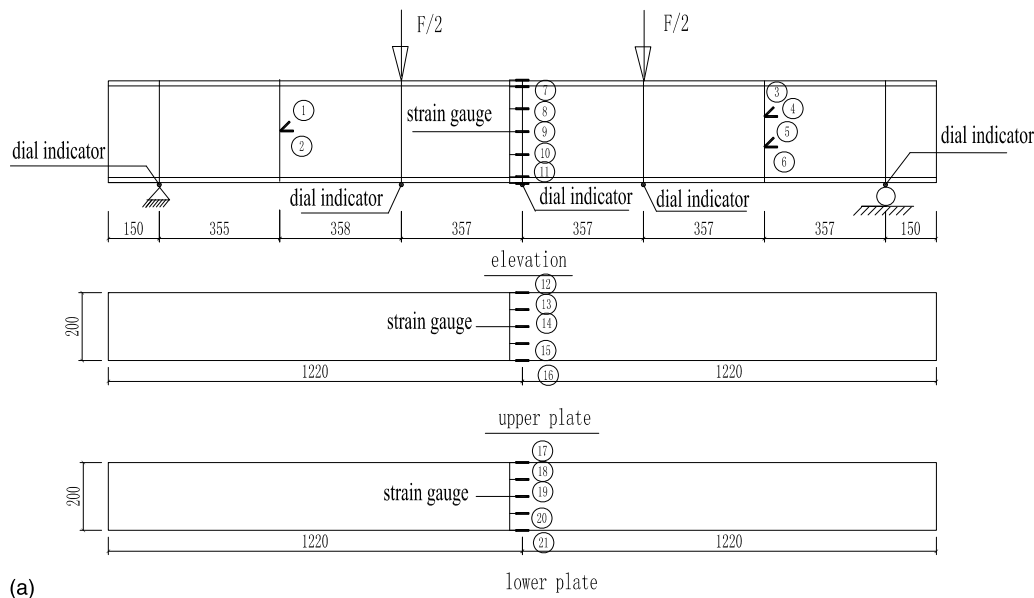


Fig. 3. Configuration of flange-web joint: (a) configuration of bolted joint; (b) detail of flange-web joint; (c) glue-line between adjacent components; (d) photo of flange-web joint (image by Wenqing Wu)

To evaluate the strength of the bolted connection in the bamboo flange-web joint and to predict the failure load based on the FEAs, the Yamada-Sun failure criterion is effective (Yamada and Sun 1978). This criterion is proposed for composite materials, and it is based on the assumption that, before total failure of the composite, every single point in the composite has failed because of cracks along the fiber according to the condition of Eq. (2):

$$e = \sqrt{\left(\frac{\sigma_1}{X}\right)^2 + \left(\frac{\tau_{12}}{S}\right)^2} \quad (2)$$

where σ_1 and τ_{12} = longitudinal and shear stress along the fibers, respectively; X = longitudinal tensile strength of the composite; and S = shear strength of the composite. Failure would occur at the point



(a)



(b) Photo of test setup

Fig. 4. Loading method of the bamboo beam and location of the gauging points: (a) arrangement of the strain gauge and dial indicator; (b) photo of test setup (image by Wenqing Wu)

where the value of e is 1. The load at the initiation of failure can be determined as when the value of e in some finite element becomes 1.

Two conditions are considered in the FEA as follows:

1. Under the deformable connection between the web and flange plates; and
2. Under the rigid connection between the web and flange plates, which is an ideal joint without connection weakening or slide deformation.

After the theoretical deformation calculation is finished by FEM, the theoretical deformation was compared with that of the experiment. The comparison of the loading-deformation curves under the experiment and the calculation is shown in Fig. 10.

Fig. 10 shows that the deflection value obtained by FEM according to the deformable connection condition is very close to the tested deflection value of Beam 2, which verified that the FEA model is effective.

The effect of the connecting way on the structural deflection was analyzed as follows.

The experimental results in Fig. 8 shows that the loading-deflection curves of all tested beams could be divided into two phases, named as

linear phase and nonlinear phase respectively, and the slope of the curve in the linear phase is bigger than that in the nonlinear phase. The fact mentioned previously shows the structural rigidity of test beam experienced a change from a higher stiffness value dropped to a lower value in the whole loading process. The fundamental reason for this phenomenon should be that the glued connection has a higher shear stiffness, plays a major role in linear phase and has a great contribution to the structural rigidity, yet in the same time the bolted connection has little contribution to the shear stiffness of the flange-web joint in the initial slip deformation (Bohnhoff and Siegel 1991). When the flexural deflection at the midspan of the test beams reached 4.7–6.2 mm, the glued connection of the I-shaped beam started cracking to failure, and the linear loading phase ended. Table 2 listed the cracking load of each test beam at the time of the glued connection cracking.

The analysis results mentioned previously can be confirmed by a comparison of the observation and calculation of the loading-deflection curve of the test beam. Using Beam 2 as an example, Fig. 10 shows that almost no difference can be observed among the initial deformation calculation with a rigid connection, the initial deformation calculation with a deformable connection, and the

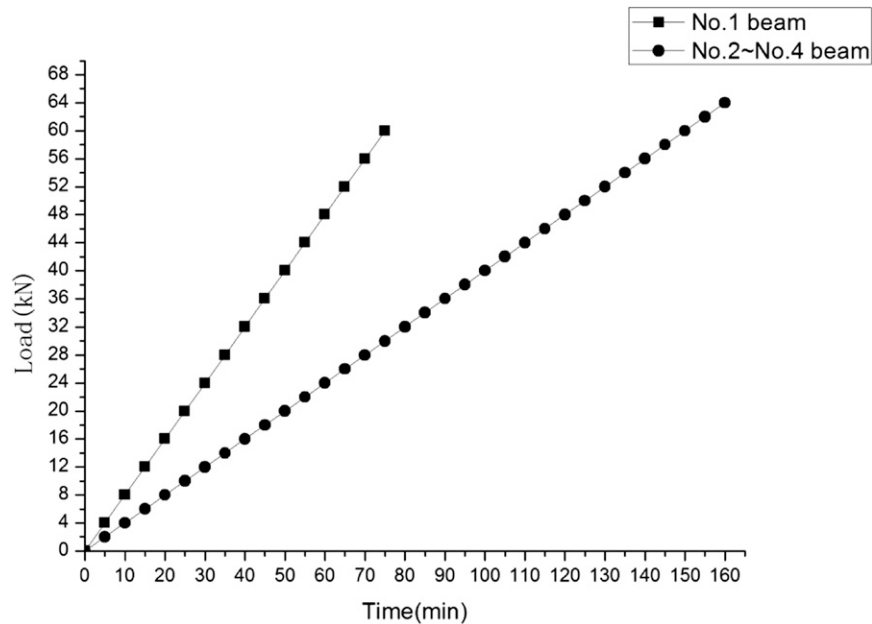


Fig. 5. Load-time curve for tested beams

observation of the initial deformation of the I-shaped beam, which verified that the glued connection of the flange-web joint has a main effect on the initial structural stiffness of the I-shaped beam, but the bolted connection had little effect on it. The initial structural deformation was in a linear phase.

After the glued connection was damaged, the mechanical bolt connection started playing a major load-bearing role, but the structural stiffness of the composite beam was reduced significantly, and then the deflection of the beam increased quickly. The relation between load and deflection was nonlinear, and the test beam performed with excellent ductility to failure.

Therefore, the glued and bolted connections can play a different role in different load-bearing phases. It was evident that the combination of two types of connections could result in a better rigidity of the test beams in the initial loading phase and also lead to a higher capacity, as well as better ductility, in the latter loading phase. In turn, based on a better understanding of the structural properties of the test beam, it is hoped that optimizing the bolted connection in quantity and in distribution will be done in the future to approach a better combination of two types of connections and to achieve a maximal cooperative action between them.

Analysis of the Relation between Variation of Deflection and Controlling Load

For the analysis of the correspondence between midspan deflection and applied load, the specific values such as midspan maximum deflection, midspan allowable deflection, allowable load, and failure load of the four beams are shown in Table 4. Because of the lack of related construction standards for bamboo structures, the reference value for allowable deflection in this work can take the value of $L/250$ as an allowable deformation under the service state according to the Code for Design of Timber Structures by China National Standard (National Standard of Peoples Republic China 2004). In this study, the value of $L/250$ equals 8.56 mm, where L is the calculated span. The corresponding allowable load can then be calculated according to the relationship between the applied load and measured deflection (Fig. 8).

Table 4 shows that the maximum experimental midspan deflection on beam failure is far beyond the allowable deflection of $L/250$ of the timber structure in the service state. Comparing the allowable deflection with the corresponding deflections in Table 3, the allowable deflection is beyond the range of the linear loading phase also, and the corresponding applied load exceeded or attained the maximum load by the end of the linear phase. After that, the structural performance entered into the early nonlinear phase under the service state. The fact mentioned previously demonstrated that the flange-web joint was not designed perfectly in this test, especially the fact that the composition of the glued connection must be modified in subsequent research on the basis of the flange-web groove joint offered in the paper by Aschheim et al. (2010) to increase the adhesive effectiveness between flanges and the web. The data in Table 4 also show that the ratio of failure load to allowable load was more than 2.0 among the different test beams, which indicated that the load-bearing structure has a high safety grade under the service state.

The test indicated that the structure deformation should be controlled effectively for the application of bamboo composite structure in bridge engineering, so improving the structural stiffness of beam will be the key point for designing this kind of beam in the future practice. Furthermore, the structural analysis results also show that the structural deformation can be controlled to a great extent if the flange-web connection can be strengthened.

Analysis of the Bending Rigidity

Based on the aforementioned analysis of the testing loading-deflection curve, the following conclusions concerning the influential factors of bending rigidity can be reached.

A glued connection has a strong effect on the bending rigidity of the I-shaped beam made of bamboo-based boards.

For example, when the load applied on Beam 2 was small in the initial testing phase, the loading-deflection curve showed a large slope and a large structural rigidity (Fig. 10). When the external load was up to 28 kN, the first inflection point appeared in the



Fig. 6. Failure mode of four test beams: (a) Beam 1; (b) Beam 2; (c) Beam 3; (d) Beam 4 (images by Wenqing Wu)

Table 2. Failure Mode and Failure Load of the Test Beams

Beam number	Failure mode	Failure type	Failure load of glued connection (kN)	Maximum failure load (kN)
1	Tearing near the bolt at the lower part of web	Tearing	22	54
2	Tearing near the bolt at the lower part of web	Tearing	28	60
3	Buckling at the upper flanges of the web	Buckling	32	64
4	Tearing near the bolt at the lower part of web	Tearing	24	56

loading-deflection curve, and the structural rigidity began to decline. All the facts mentioned previously indicate that the epoxy resin structural adhesive in the flange-web joint began to locally fail. When the load was up to 44 kN, the curve slope decreased significantly, and the deflection increased more quickly. At this time, most of the glued connection had failed, and the structural rigidity decreased to a lower level. This finding indicated that the bending

rigidity of the bamboo composite I-shaped beam was apparently affected by an action of the flange-web gluing connection. Therefore, this study shows that if the construction quality of the glued connection can be guaranteed so that the I-shaped beam would work under normal service conditions and the glued connection would not easily fail, then the bending rigidity of the I-shaped beam made of bamboo plywood can be markedly improved.



(a)



(b)

Fig. 7. Typical external features of test beam failure: (a) Beam 1; (b) Beam 2 (images by Wenqing Wu)

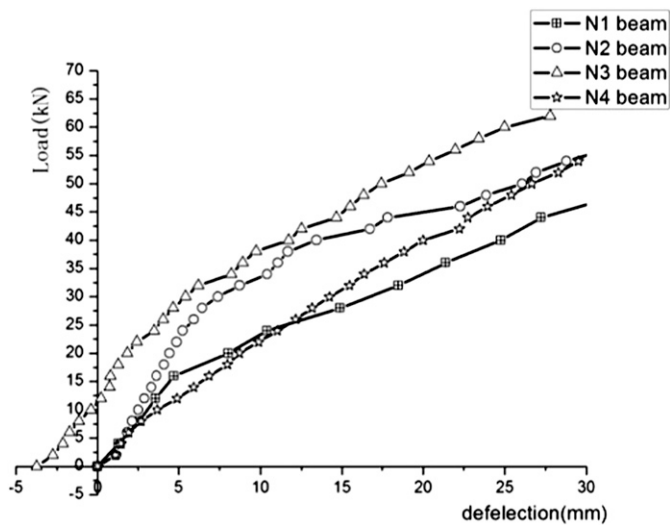


Fig. 8. Load-deflection experimental curve of test beam

Table 3. Phase Classification of the Load-Deflection Curves of Four Beams

Beam number	External load range (kN)		Deflection range (mm)	
	Linear stage	Nonlinear phase	Linear phase	Nonlinear phase
1	0–16	16–54	0–4.72	4.72–36.94
2	0–28	28–60	0–6.43	6.43–31.82
3	0–32	32–64	0–6.19	6.19–27.77
4	0–12	12–56	0–5.10	5.10–29.52

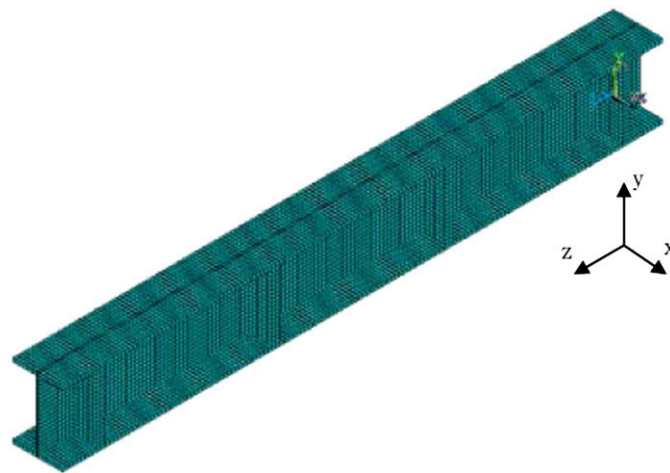


Fig. 9. ANSYS FEA analysis model of test beam

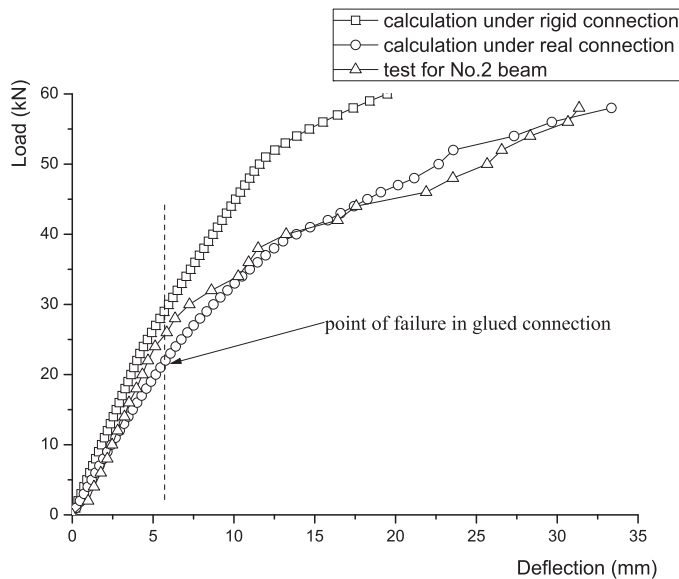


Fig. 10. Comparison between observation and calculation of load-deflection curve in Beam 2

The number of connecting bolts also greatly influences the bending rigidity of the structure. In addition, Fig. 10 shows that strengthening the connection can effectively reduce the bending deformation of the structure at a later phase. Therefore, improving the quality of the glued and bolted connections is also very important.

The influence of the external rebar on the bending rigidity of the beam is small. Comparing the deflection difference between Beam 4 with nonprestressing rebar and Beams 1 and 2 without external

Table 4. Relationship between Maximum Midspan Deflection and Load of Four Beams

Beam number	Maximum deflection (mm)	Deflection/span ratio	Failure load (kN)	Allowable deflection (L/250) (mm)	Allowable load (kN)	Failure load/allowable load
1	36.94	1/58	54	8.56	21.0	2.6
2	31.82	1/67	60	8.56	30.0	2.0
3	27.77	1/77	64	8.56	29.5	2.2
4	29.52	1/72	56	8.56	21.2	2.6

rebar, the deflection increase of Beam 4 was between that of Beams 1 and 2, which demonstrated that the external nonprestressing rebar did not improve the bamboo I-shaped beam with respect to bending rigidity (Fig. 8).

The influence of external prestressing on the bending rigidity of the beam is also limited. At the linear phase, the slope of the loading-deflection curve of Beam 2 was consistent with that of Beam 3 with external prestressing (Fig. 8). The cross-sectional bending rigidity of both Beams 2 and 3 at the linear phase was very close, which illustrated that the external prestressing has a limited contribution to the bending rigidity of the bamboo I-shaped beam. However, the total flexural deformation was small under the same loading conditions for Beam 3 with the external prestressing caused by the presence of pre-camber.

Tensile Test Results and Analysis of the External Rebar

The initial tensile force of Beam 3 with the external prestressing rebar was 22 kN. The effective tensile forces of the prestressing rebar in different times were measured before the loading procedure to attain the short-term prestress loss of the external prestressing rebar. The test results are shown in Table 5.

The data show that when the external prestressing rebar in the bamboo beam structure was tensioned with a tensile force for 72 h, the tensile force on the rebar was reduced by approximately 2.7%, which is just a small prestressing loss. Thus, the rebar can meet the load-bearing requirements.

During the test process, the effective tensile force on the rebar in Beams 3 and 4 was also measured, and the results are shown in Fig. 11. There was an initial tensile force of 1.7 kN in the external rebar of Beam 4 for the fastening rebar. The test analysis showed the following conclusions:

- When Beam 3 failed, the increment of the tensile force in the installed rebar was just 2.2 kN, which is approximately 10% of the initial tensile force, and the tensile force of the rebar is considered to have a small change;
- When Beam 4 failed, the increment of tensile force in the installed rebar was up to 6.0 kN, which is also a small change; and
- When the beam was damaged, a yield failure was not observed in the external rebar of Beams 3 and 4 because of the small change in the tensile force of two beams.

Analysis on Cross-Sectional Strain Variation

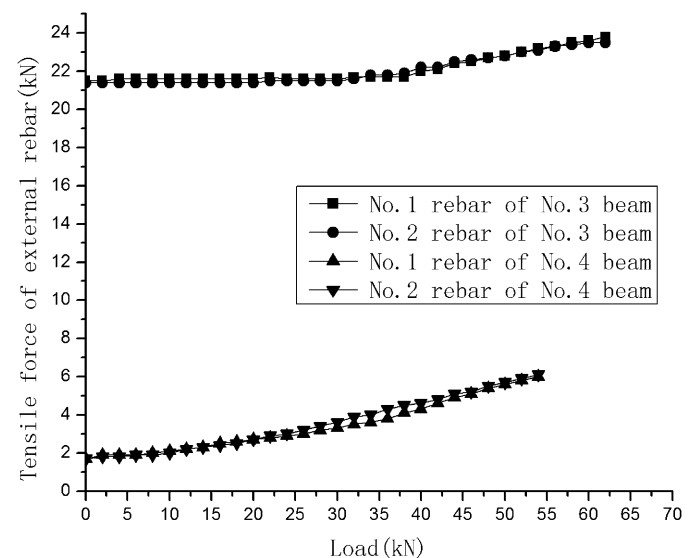
The five strain values of the strain measuring points on the web at the midspan cross section of four beams are shown in Fig. 12, which illustrates the strain distribution on the web along the depth of the cross section.

Figs. 12(a-d) show the following conclusions.

During the linear loading process, the longitudinal strain of the web at the midspan cross section showed a linear distribution along

Table 5. Tensile Force Changes of the External Prestressed Rebar in Beam 3

Time point (h)	No. 1 rebar (kN)	No. 2 rebar (kN)
0	22.1	22
24	21.6	21.4
48	21.5	21.4
72	21.5	21.4

**Fig. 11.** Tensile test of external rebar

the cross-sectional depth, indicating that the strain at the midspan cross section approximately agreed with the plane section assumption. After the glued connection fails, however, the longitudinal strain of the web at the midspan cross section was not in a linear distribution along the cross-sectional depth, because of the imperfect design of the flange-web joints.

As the load increased, the strain curve had a sharp increasing phase in the web strain. The reason was that the glued connection, as one of the structural connections, was damaged and then eventually failed, accompanied by structural rigidity changes. The reason for this failure was similar to that of the apparent changes in the aforementioned midspan deflection.

Beam 3 was previously subjected to longitudinal prestress. Thus, under the same load, the longitudinal tensile strain at the downside of the midspan section of Beam 3 was smaller than that of the other beams. Moreover, the final structural failure was caused by the excess compressive strain of the upper web, which led to local buckling of the structure and failure of the beam. This phenomenon may explain why the failure mode of Beam 3, after being subjected to external prestressing, was different from that of the other beams.

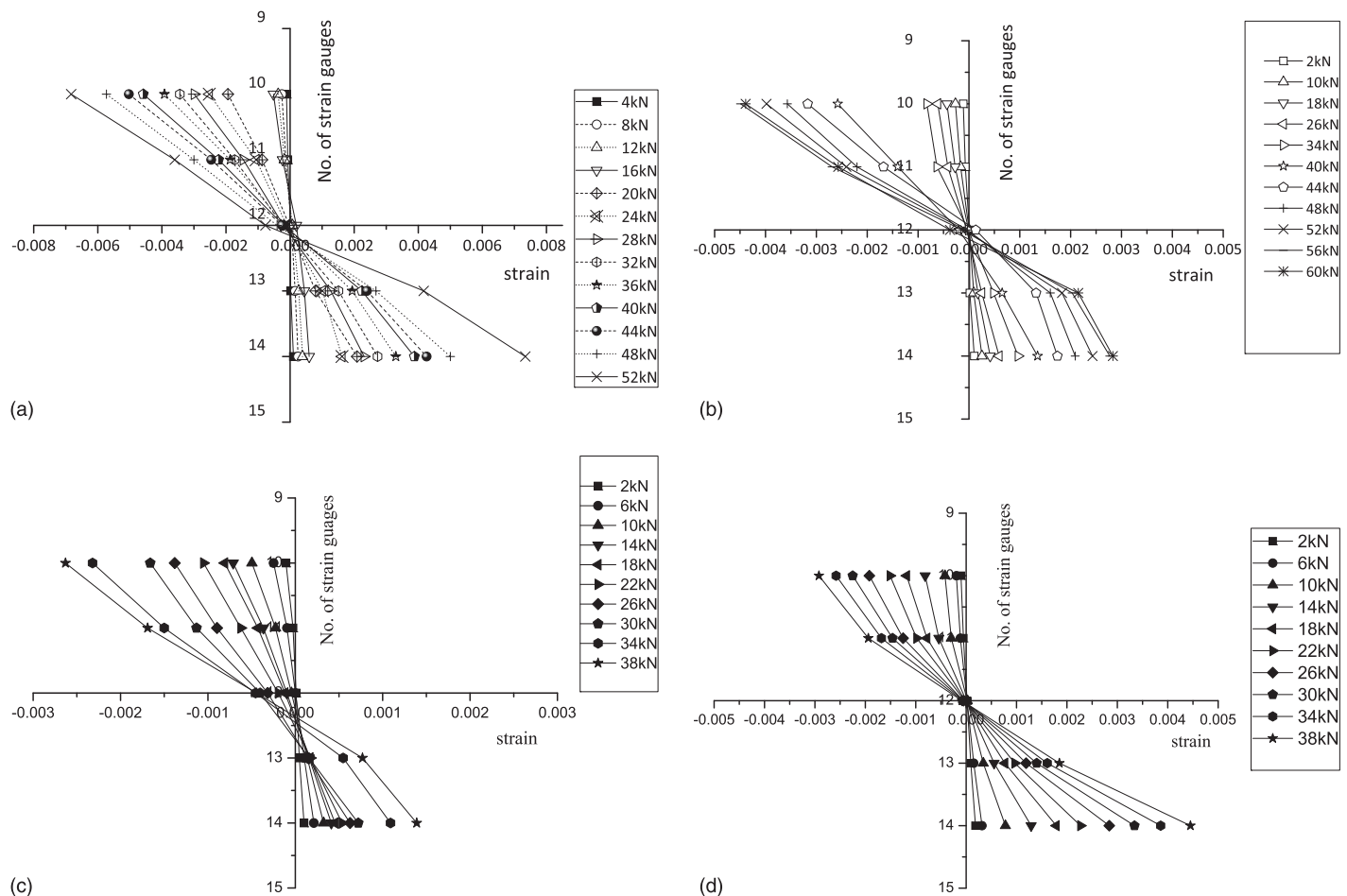


Fig. 12. Web strain changes of four beams at the midspan cross section: (a) Beam 1; (b) Beam 2; (c) Beam 3; (d) Beam 4

In terms of the longitudinal strain distribution mode along the width of the top/bottom plates, Figs. 13(a and b) show the strain curve of the five strain measuring points on the top and bottom plates at the midspan cross section of Beam 2.

Fig. 13 shows the following conclusions.

The measuring points of the longitudinal strain were not uniformly distributed along the width of the plates. Rather, they were distributed in a pattern of large at the middle and small at the two ends. The longitudinal stress distribution of the top and bottom plates presented obvious shear lag effects.

Similar to the longitudinal strain variation of the web, the strain curve had a sharp increasing phase in the strain of the top and bottom plates when the load value ranged from 38 to 40 kN. At this time, the bending rigidity of the structure was reduced, and the structural integrity also declined. As a result, the glued connection started to be damaged and eventually failed.

In this work, only four beams were tested under one loading type, and out of them, only two are of the same type. The number of the test beams is of a serious deficiency in this paper, so spread of strength properties, failure load and mode as well as bending rigidity performance of bamboo composite I-shaped beam has a limitation in representativeness of mechanical performance of its kind. It is hoped that more experiments on test beams are done in the future to better understand the mechanical performance of this kind of beam.

The experimental results also show that there are several imperfections in the geometrical shape, e.g., the thickness of web is not sufficient to withstand the tearing action of the imbedded shear

stress of the bolt shank, because of the small ratio of the thickness of the web to the diameter of bolt, and the thickness of the web is also not sufficient to ensure that the web doesn't buckle when it fails. Conversely, the design of the flange-web joint also has some imperfections, e.g., it is better if the glued connection uses a grooved style glued joint.

Conclusion

The glued and bolted flange-web connections of the bamboo composite I-shaped beam can play a different role in different load-bearing phases, respectively. It is evident that the combination of two type of connections can result in a better rigidity of the test beam in the linear loading phase and can also lead to a higher capacity and better safe ductility in the nonlinear loading phase.

Optimizing the mechanical connections in quantity and its distribution is necessary to maximize the cooperative action between the two types of connection ways.

Applying an external prestressing action on the bamboo composite beam can also help improve the structural stress state in web and reduce the whole deformation of the beams. However, the function of external prestressing for improving structural rigidity and bending capacity of the beams is limited.

In the linear loading process, the longitudinal strain distribution along the depth of the web at the midspan cross section is approximately linear, which indicated that the plane cross section assumption for elementary theory of beams can be taken as a basic

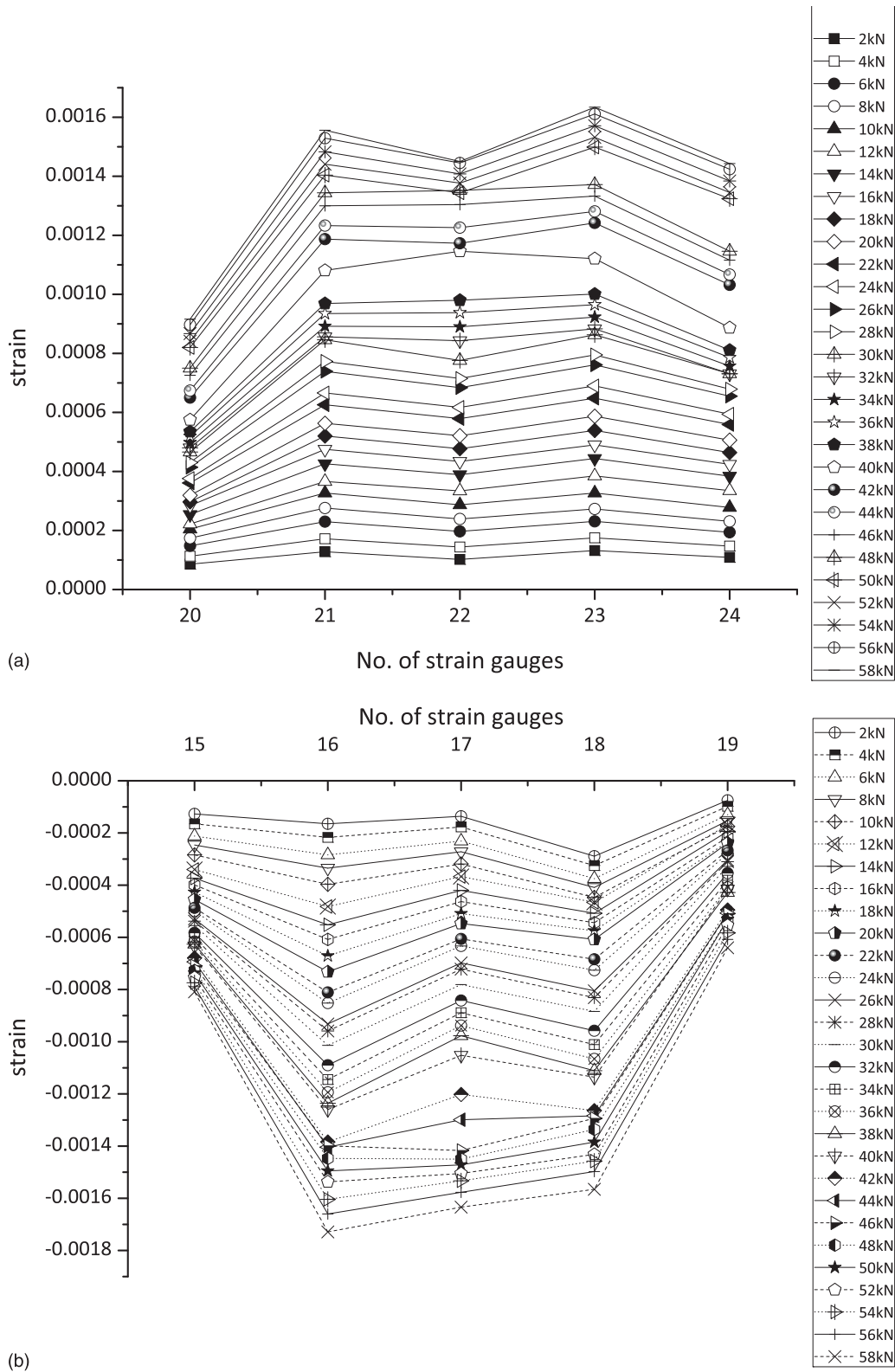


Fig. 13. Strain distribution of up/bottom flange plate of Beam 2 at the midspan: (a) strain distribution of the top plate; (b) strain distribution of the bottom plate

assumption in calculation of normal stress in the bamboo composite I-shaped beam.

The test achievement indicated that the structure deformation should be controlled effectively for the application of bamboo composite structure in bridge engineering, so improving the structural

stiffness of the beam will be the key point of this kind of beam design.

The structural security is high if the structure is under a service state, and the bearing capacity may be remarkable when the structure is damaged.

References

- Ahmad, M., and Kamke, F. A. (2005). "Analysis of Calcutta bamboo for structural composite materials: Physical and mechanical properties." *Wood Sci. Technol.*, 39(6), 448–459.
- Amino, Y. (2004). "Bamboo-precocious wood composite beams: Theoretical prediction of the bending behaviour." *J. Bamboo Rattan*, 3(2), 107–121.
- Amino, Y. (2005). "Bamboo-precocious wood composite beams: Bending capacity for long-term loading." *J. Bamboo Rattan*, 4(1), 55–70.
- ANSYS 10.0 [Computer software]. Canonsburg, PA, Ansys.
- Aschheim, M., Gil-Martín, M. L., and Hernández-Montes, E. (2010). "Engineered bamboo I-joists." *J. Struct. Eng.*, 10.1061/(ASCE)ST.1943-541X.0000235, 1619–1624.
- Bahari, S. A., Ahmad, M., Nordin, K., and Jamaludin, M. A. (2010). "Tensile mechanics of bamboo strips." *AIP Conf. Proc.*, 1217, 457–461.
- Bohnhoff, D. R., and Siegel, C. E. (1991). "Bending strength and stiffness of wood I-beams with nail and elastomeric adhesive bonding." *Trans. ASAE*, 34(1), 259–268.
- Buchanan, A., et al. (2008). "Multi-storey prestressed timber buildings in New Zealand." *Struct. Eng. Int.*, 18(2), 166–173.
- Gao, L., Wang, Z., and Chang, L. (2008). "Performance and application study of bamboo composite material in building structures." *World Bamboo Rattan*, 6(6), 1–5.
- Iqbal, A., et al. (2008). "Seismic behaviour of prestressed timber columns under bi-directional loading." *Proc., 10th World Conf. on Timber Engineering*, Vol. 4, Springer, Netherlands, 1810–1817.
- Janssen, J. J. A. (1981). "Bamboo in building structure." Ph.D. thesis, Eindhoven Univ. of Technology, Faculty of Architecture, Building and Planning, Eindhoven, Netherlands.
- Jorissen, A. J. M., Voermans, J., and Jansen, M. H. (2007). "Glued-laminated bamboo: Node and joint failure in bamboo laminations in tension." *J. Bamboo Rattan*, 6(3–4), 137–144.
- Kumar, V. K., Stern, E. G., and Szabo, T. (1972). *Built-up and composite beams*, Virginia Polytechnic Institute and State Univ., Blacksburg, VA, 24.
- Lee, A. W. C., Bai, X., and Peralta, P. N. (1994). "Selected physical properties of giant timber bamboo grown in South Carolina." *For. Prod. J.*, 44(9), 40–46.
- Leichti, J. R., Falk, H. R., and Laufenberg, L. T. (1990). "Prefabricated wood composite I-beams: A literature review." *J. Wood Fiber Sci.*, 2(1), 62–79.
- Ma, X. Y. (2013). "Experimental study on the mechanical performance of shear-connector in I-shaped bamboo composite beam." M.S. thesis, Southeast Univ., Dept. of Transportation, Nanjing, China.
- Nath, A. J., Das, G., and Das, A. K. (2009). "Above ground standing biomass and carbon storage in village bamboos in North East India." *Biomass Bioenergy*, 33(9), 1188–1196.
- National Standard of Peoples Republic China. (2001). "Code for design of steel structure." *GB 50009-2001*, Beijing.
- National Standard of Peoples Republic China. (2004). "Code for design of timber structures." *GB 50005-2003*, Beijing.
- Rittironk, S., and Elnieiri, M. (2008). "Investigating laminated bamboo lumber as an alternate to wood lumber in residential construction in the United States." *Proc., 1st Int. Conf. on Modern Bamboo Structures*, Y. Xiao, M. Inoue, S. K. Paudel, eds., CRC Press, Boca Raton, FL, 83–96.
- Sawata, K., and Yasumura, M. (2003). "Estimation of yield and ultimate strengths of bolted timber joints by nonlinear analysis and yield theory." *J. Wood Sci.*, 49(5), 383–391.
- Shan, B., Zhou, Q., and Xiao, Y. (2009). "Research and application of modern bamboo structure technology in pedestrian overpass." *J. Hunan Univ.*, 36(10), 29–35.
- Shen, Z. R., Ni, Y., and Hu, Z. L. (2009). "Material test and structural analysis of 'Germany and China, together in movement' bamboo structure exhibition hall." *Struct. Eng.*, 25(1), 51–54.
- Smith, T., et al. (2008). "Design and construction of prestressed timber buildings for seismic areas." *Proc., 10th World Conf. on Timber Engineering 2008*, Vol. 4, Springer, Netherlands, 1746–1753.
- Sulastiningsih, I. M., and Nurwati, A. (2009). "Physical and mechanical properties of laminated bamboo board." *J. Trop. For. Sci.*, 21(3), 246–251.
- Sun, Z. J., Cheng, Q., and Jiang, Z. H. (2008). "Manufacturing methods and performance of bamboo engineering materials." *J. Compos. Mater.*, 24(1), 80–83.
- Tsai, S. W., and Wu, E. M. (1971). "A general theory of strength for anisotropic materials." *J. Compos. Mater.*, 5(1), 58–80.
- Van der Lugt, P., Van den Dobbelen, A. A. J. F., and Janssen, J. J. A. (2006). "An environmental, economic and practical assessment of bamboo as a building material for supporting structures." *Construct. Build. Mater.*, 20(9), 648–656.
- Wei, Y., Zhang, Q. S., Jiang, S. X., and Lü, Q. F. (2011). "Basic properties and application prospects of new bamboo materials in building structures." *Archit. Technol.*, 42(5), 390–393.
- Wu, W. Q., Chen, S., and Ma, X. Y. (2012a). "Test research on flexural and shear properties of bamboo plywood." *Appl. Mech. Mater.*, 166–169, 2951–2957.
- Wu, W. Q., Ma, X. Y., and Chen, S. (2012b). "Experimental study on the compressive mechanical performance of bamboo strip plywood under static loads." *Adv. Mater. Res.*, 598, 640–646.
- Wu, W. Q., Ma, X. Y., and Chen, S. (2012c). "Feasibility study of bamboo strip plywood used in structure engineering." *Proc., 4th Asia-Pacific Young Researchers and Graduates*, Hong Kong, 236–243.
- Xiao, Y., Yang, R. Z., Shan, B., She, L. Y., and Li, L. (2012). "Experimental research on mechanical properties of glulam." *J. Building Struct.*, 33(11), 150–157.
- Xiao, Y., Zhou, Q., and Shan, B. (2010). "Design and construction of modern bamboo bridges." *J. Bridge Eng.*, 10.1061/(ASCE)BE.1943-5592.0000089, 533–541.
- Yamada, S. E., and Sun, C. T. (1978). "Analysis of laminate strength and its distribution." *J. Compos. Mater.*, 12(3), 275–284.
- Yu, H. Q., Jiang, Z. H., Hse, C. Y., and Shupe, T. F. (2008). "Selected physical and mechanical properties of Moso bamboo (*Phyllostachys pubescens*)." *J. Trop. For. Sci.*, 20(4), 258–263.
- Yu, H. Q., Jiang, Z. H., Ren, H. Q., and Fei, B. H. (2006). "The mechanical properties and the resistance to aging of the parallel bamboo curtain laminated panels." *J. Wood Working Mach.*, 3(1), 1–4.
- Zhang, Y. T., and He, L. P. (2007). "Mechanical performance comparison between laminated bamboo and common building materials." *J. Zhejiang For. Coll.*, 24(1), 100–104.
- Zhang, Y. T., and Yue, H. (2004). "Artificial bamboo board—An ideal engineering structure material." *Archit. Technol.*, 4(4), 17–18.